Hindawi Publishing Corporation
Journal of Sensors
Volume 2016, Article ID 1353212, 8 pages
http://dx.doi.org/10.1155/2016/1353212

Research Article

Detailed Analysis of the Timing Measurements in Optical Position Sensing Devices Based on Laser Beam Deflection

Andreas Tortschanoff

Carinthian Tech Research AG, Europastrasse 12, 9524 Villach, Austria

Correspondence should be addressed to Andreas Tortschanoff; andreas.tortschanoff@ctr.at

Received 30 August 2015; Accepted 23 November 2015

Academic Editor: Marco Consales

I present a detailed analysis of the timing signals observed, when measuring the oscillation of a Lissajous scanner by sending a reflected laser beam onto carefully placed trigger diodes. This technique was used in a device which we have developed recently for the measurement of resonant MEMS scanner mirrors. For 2D scanner mirrors, cross talk between the two axes is observed. This cross talk can be well understood theoretically. In this paper, a quantitative analytical description is presented, which is confirmed by experimental results.

1. Introduction

There is increasing interest in MOEMS (microoptoelectromechanical systems) [1] based devices, which can provide miniaturized, robust, and potentially cheap solutions in order to meet the demands of the current consumer market [2–5]. Electrostatically driven resonant scanner mirrors are an important class of MOEMS devices [5, 6]. Providing position feedback for such MOEMS mirrors is crucial for many applications and, in particular, position feedback is necessary for closed loop operation [7].

Position feedback can be realized by measuring a laser beam reflected from the backside of the mirror. This is a very versatile approach and, in recent work, we presented two devices capable of driving resonant 1D and 2D MOEMS scanner mirrors [8, 9]. In both devices, the angular position of the mirror is encoded by an optical trigger signal combined with a harmonic extrapolation function. In combination with appropriate driver electronics, they can provide closed loop control and ensure stable mirror oscillation under varying environmental conditions.

For 2D MOEMS mirrors, we used cylindrical mirrors in order to suppress the deflection of the orthogonal dimension. The backside of the mirror reflects two crossed orthogonal laser beams, whose reflections pass a cylindrical mirror before being sent onto the photodiodes for the timing signals. This reduces the problem to the control of two independent 1D oscillations and allows accurate position sensing and closed loop control.

Some details have to be considered in this case. In particular, there is some remaining cross talk between the axes, which results from the projection onto a plane surface of the detectors. In the following we shortly review the position encoding and feedback scheme implemented in the 2D device and then focus on these artefacts in much detail.

2. Description of the System

2.1. System Description. The whole position detection system is integrated in a detector head with a size of 20 × 15 × 15 mm^2 as shown in Figure 1(a). Details are described in [9]. Micromechanical scanner mirrors from the Fraunhofer IPMS were investigated in our modules [10–13]; but also other electrostatically driven MEMS scanner mirrors could be used, if they are optically accessible from the backside.

Figure 1(b) shows the demonstrator setup where the beam from a laser pointer is reflected from the 2D module projecting a Lissajous figure onto a screen. This setup was used in our experiments.

In the module, the delay between successive passages of the reflected laser beam on a fast detection diode is

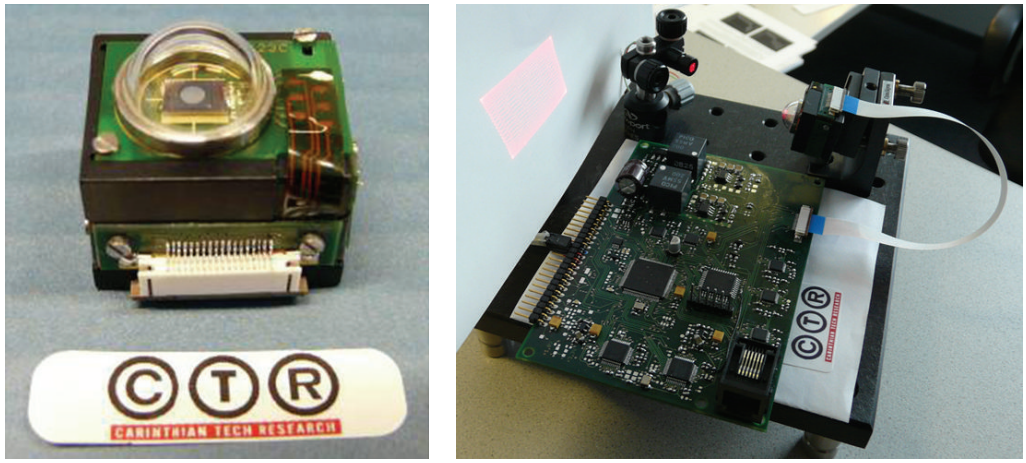

(a) (b)

Figure 1: (a) Photo of our module with integrated position detection. (b) Demonstrator setup.

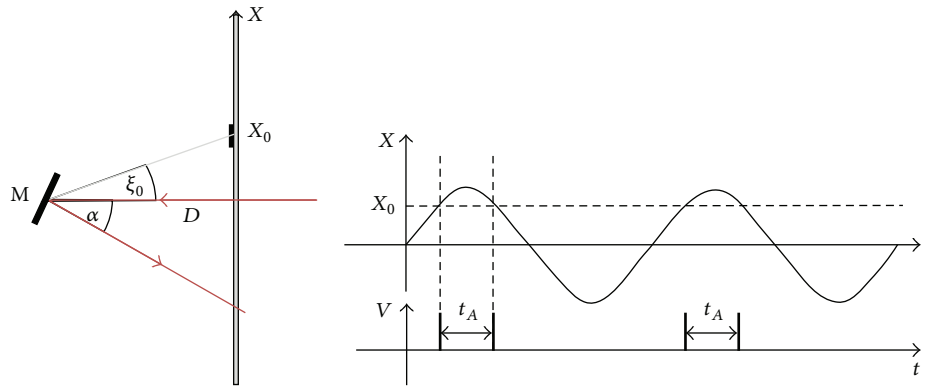

(a) (b)

Figure 2: (a) Scheme for the optical measurement of the amplitude for a single axis. (b) The corresponding signals (see text for details).

measured. From this time delay, the amplitude and phase of the mirror oscillation can be deduced, assuming purely sinusoidal motion. The scheme is illustrated in Figure 2.

A fast photodetector at position X_0 measures the timing of the passage at a fixed angular deflection angle ξ_0. The delay between two consecutive trigger signals t_A allows calculation of the amplitude.

As a side remark, note that, to completely characterize the oscillation, also the phase should be determined (e.g., with regard to some mirror driving signal). The phase information can also be retrieved from the amplitude diode, since, for sinusoidal motion, the maximum of the signal is located exactly midway between the two trigger signals from the amplitude diode. Higher precision is obtained by using an additional dedicated diode, situated exactly at zero-deflection angle. In the following, we only focus on amplitude information.

This approach can also be used with 2D MOEMS devices but this implies a significant increase in complexity, because we have to characterize a 2D Lissajous figure instead of a straight line.

In order to apply the same approach, we could use a rectangular photodiode, which covers one dimension completely and still is very thin in the other direction. Alternatively, we can compress one direction using cylindrical optics (see Figure 3). Mirror deflection around one axis is compensated at the plane of the detection diode while deflection around the other axis still leads to a horizontal deflection. This reduces the problem to the measurement of two individual 1D oscillations and allows accurate position sensing and closed loop control for this axis.

More specifically, in our device, the backside of the mirror is hit by two crossed orthogonal laser beams, and each reflected beam passes a cylindrical mirror before being sent onto the photodiodes for the timing signals. Thus, the problem is reduced to the control of two 1D oscillations.

Strictly speaking, the compensation of the oscillation with cylindrical optics is not perfect. Elliptical or toroidal mirrors could provide higher accuracy. However, even in the case of ideal optics, exact compensation of the distortion of the deflection of one axis is only provided at zero deflection of the other, because of the projection of the beam onto a planar

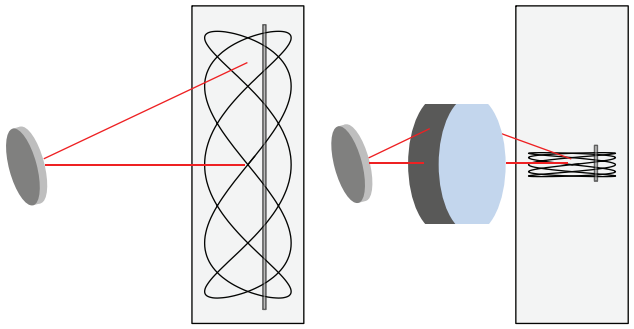

Figure 3: (a) A 2D scanner projects a Lissajous pattern. In order to detect the horizontal deflection, a high photodetector would be necessary. (b) In order to measure one axis using the same detection scheme as in the 1D case, the other axis can be compressed using cylindrical optics.

surface. This results in a small variation of the timing of the amplitude diode as a function of the deflection around the orthogonal axis. This leads to a timing artefact, which will be described in detail in the remainder of the paper.

2.2. Position Detection. If we assume a 1D mirror oscillating around a single axis, we can describe its tilt angle α as a sinusoidal function in time, with amplitude A and angular frequency ω:

$$\alpha = A \sin(\omega t). \tag{1}$$

From the amplitude delay, that is, the time delay t_A between two successive signals from the amplitude diode, it is straightforward to calculate the amplitude A of the oscillatory mirror motion, if the angular position ξ_0 of the diode is known (see Figure 2):

$$A = \frac{\xi_0}{\sin\left(\pi\left(1/2 - t_A/T\right)\right)}. \tag{2}$$

If the linear position X_0 of the detector is given, we have to use the relation that $\tan(\xi_0) = X_0/D$, where D is the distance of the plane of detection from the scanner mirror. The expression for the amplitude in this case becomes

$$A = \frac{\tan^{-1}\left(X_0/D\right)}{\sin\left(\pi\left(1/2 - t_A/T\right)\right)}. \tag{3}$$

To minimize the error, it is advantageous to position the reference diode for the amplitude at a rather high deflection angle. On the other hand, ξ_0 defines the minimal angle, where measurement and amplitude control are possible. A good compromise is to place the amplitude diode at about half the maximal deflection angle expected during operation.

While this works fine for a single axis of rotation, artefacts are introduced by the projection of the gimbal mounted 2D devices. These distortion effects result from the projection onto a plane surface, as illustrated in Figure 4. Assuming a

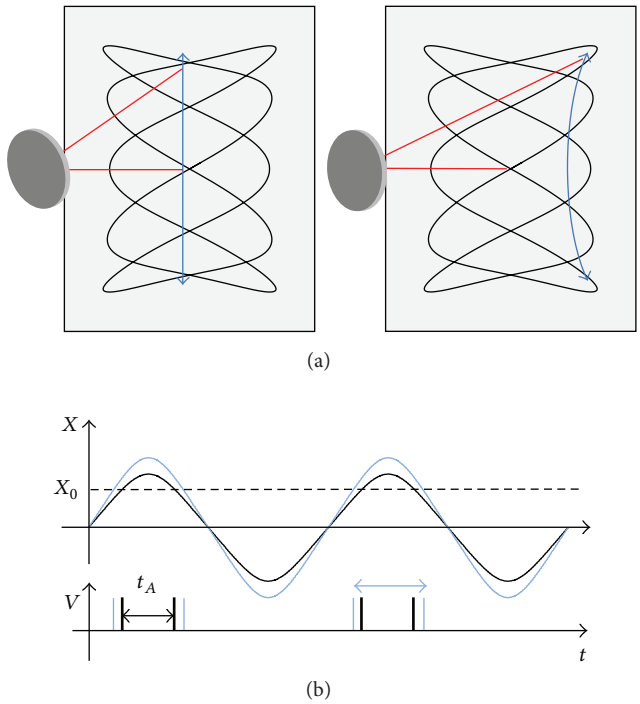

Figure 4: Deflection around the orthogonal axis also influences the height of the projection onto a plane observed around the orthogonal direction. This influences the measured delay for calculating the amplitude.

mirror, which is oscillating harmonically around a single axis, we obtain a characteristic deflection curve of the reflected laser beam, which critically depends on the deflection around the orthogonal axis. Deflection around the orthogonal axis changes the curve of the deflected laser beam and leads to deviations in the values of the timing signals. The situation is even more complex for a mirror oscillating around both axes simultaneously and a more detailed analysis is required, if one wants to use the timing signals for amplitude determination. This will be analyzed in detail in the following sections.

3. Mathematical Analysis

In this section, we will give a quantitative description of the timing signals.

The definitions we use are depicted in Figure 5. We assume a gimbal mounted scanner mirror whose springs are aligned horizontally parallel to the y-axis of the global coordinate system. The axis of rotation of the mirror-frame is the vertical axis, parallel to the z-axis of the global coordinate system. We also name the inner axis and the axis of the frame as "fast axis" and "slow axis," respectively, since, in general, the resonance frequency around the inner axis is higher because of the additional mass of the frame. This can be reversed if the spring constants of the two axes are very different, which is a design parameter of the MEMS mirrors.

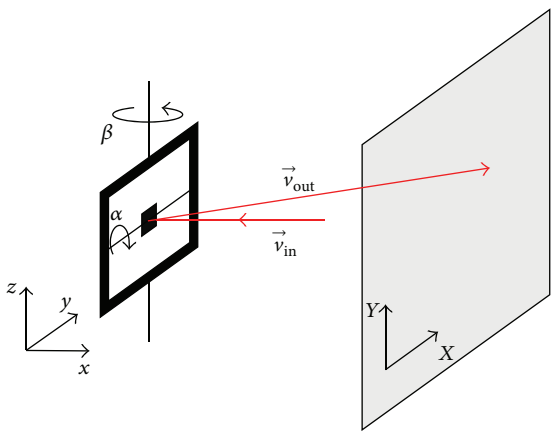

FIGURE 5: Scheme of the geometry and definition of the relevant parameters. Note that the axes of the global coordinate system are labelled with x, y, z and the local frame of reference of the screen uses coordinates X and Y, as indicated in the scheme.

The mirror orientation is characterized by the normal vector $\vec{m}$ of the mirror plate. In terms of the deflection angles α, β of the individual axes, it can be expressed as

$$\vec{m} = \begin{pmatrix} \cos(\alpha)\cos(\beta) \\ \cos(\alpha)\sin(\beta) \\ \sin(\alpha) \end{pmatrix}. \tag{4}$$

In the most general case, we have a laser beam with arbitrary direction, which is reflected from the mirror. Its direction is described by the vector $\vec{v}_{in}$:

$$\vec{v}_{in} = \begin{pmatrix} -\cos(\delta)\cos(\gamma) \\ \cos(\delta)\sin(\gamma) \\ \sin(\delta) \end{pmatrix}. \tag{5}$$

Here γ and δ are the angles of the beam defined in the same way as α and β.

In this general case, after some simple algebra, the reflected beam can be expressed as

$$\vec{v}_{out} = \begin{pmatrix} (2\cos\alpha\cos\beta\cos\gamma\cos\delta - 2\cos\alpha\sin\beta\sin\gamma\cos\delta - 2\sin\alpha\sin\delta)\cos\alpha\cos\beta - \cos\delta\cos\gamma \\ (2\cos\alpha\cos\beta\cos\gamma\cos\delta - 2\cos\alpha\sin\beta\sin\gamma\cos\delta - 2\sin\alpha)\sin\delta\cos\alpha\cos\beta + \cos\delta\cos\gamma \\ (2\cos\alpha\cos\beta\cos\gamma\cos\delta - 2\cos\alpha\sin\beta\sin\gamma\cos\delta - 2\sin\alpha\sin\delta)\sin\alpha + \sin\delta \end{pmatrix}. \tag{6}$$

For the remaining discussion in this paper, we will only deal with the special case that the incoming beam is hitting the mirror orthogonally to its rest position ($\delta = \gamma = 0$). Thus we assume an incoming beam

$$\vec{v}_{in} = \begin{pmatrix} -1 \\ 0 \\ 0 \end{pmatrix}. \tag{7}$$

In this case, the reflected beam can be written as

$$\vec{v}_{out} = \begin{pmatrix} 2\cos^2\alpha\cos^2\beta - 1 \\ \cos^2\alpha\sin(2\beta) \\ \cos\beta\sin(2\alpha) \end{pmatrix}. \tag{8}$$

In a first approximation, this could be approximated by $\vec{v}_{out}^{(1)} = \begin{pmatrix} 1 \\ 2\beta \\ 2\alpha \end{pmatrix}$. In this case, the cross talk between the two axes vanishes and the correct amplitude can be obtained using (2) or (3). However, this approximation only holds for very small angles of deflection and, here, we want to discuss the more general case, going beyond the first approximation.

The position, where the reflected beam hits a screen which is placed at a distance d (and orthogonal to the direction of the reflected beam), can be expressed as

$$\begin{aligned} \begin{pmatrix} X \\ Y \end{pmatrix} &= d \begin{pmatrix} \dfrac{\cos^2\alpha\sin(2\beta)}{2\cos^2\alpha\cos^2\beta - 1} \\ \dfrac{\cos\beta\sin(2\alpha)}{2\cos^2\alpha\cos^2\beta - 1} \end{pmatrix} \\ &= d \begin{pmatrix} \dfrac{\sin(2\beta)}{\cos(2\beta) - \tan^2\alpha} \\ \dfrac{\sin(2\alpha)}{\cos\beta\cos(2\alpha)} \end{pmatrix}, \end{aligned} \tag{9}$$

where we labelled the horizontal and vertical axis on the screen with X and Y, respectively. (Note that, for the case of zero angle of incidence, which is discussed here, the X and Y coordinates of the screen are parallel to y and z of the coordinate system of the mirror.)

In the following, we will quantitatively discuss its influence on our detection system. First we consider the case were one axis is statically actuated and finally also the case where both axes are oscillating. In particular, we will estimate the influence on the outcome of the timing measurements, which we use in our devices for the determination of the mirror's oscillation amplitude.

3.1. Static Deflection. For the mathematical treatment, we assume a Lissajous pattern projected onto a flat screen and a detector, which measures the timing, when the beam hits a certain X- or Y-position on this screen (c.f. Figure 3(a)).

Starting with the horizontal deflection, we assume that the detector is placed at a position X_0. If there is no deflection of the second axis ($\alpha = 0$), this detector is hit when the deflection of the vertical axis has an angle of β_0 and the following relation holds:

$$X_0 = d\tan(2\beta_0). \tag{10}$$

If the other axis is tilted at an arbitrary angle α, the detector will actually be hit at a slightly different mirror deflection angle β_α:

$$\frac{\sin(2\beta_a)}{\cos(2\beta_a) - \tan^2\alpha} = \frac{X_0}{d}. \tag{11}$$

This angle is shifted by an amount $\Delta_\beta = \beta_a - \beta_0$ with regard to β_0. It is easy to show that for small shifts $\Delta_\beta \sim -(1/2)\sin(2\beta_0)\tan^2\alpha$. Δ_β is negative, meaning that the detector is hit "earlier" (at smaller angles β) for any finite deflection of the orthogonal axis α compared to the reference case $\alpha = 0$.

This deviation directly leads to an error in the measured time delay t_A (see Figure 4(b)) which is the quantity which is used for the amplitude determination. This timing error Δ_t depends on the angular velocity v of the mirror when crossing the detector (i.e., at an angle $\beta = \beta_\alpha$):

$$\Delta_t = -\frac{2\Delta_\beta}{v}. \tag{12}$$

(The factor of −2 results from the fact that t_A is the time difference of the two trigger signals (see Figure 4).) As a consequence, it depends on the position of the detector X_0 as well as the actual amplitude and frequency of the mirror motion.

For illustration, we assume that the detector is placed at half the amplitude of deflection ($\beta_0 = A_\beta/2$). In this case, we know that $\omega_\beta t_0 = \pi/6$ and can deduce the velocity of the mirror deflection as $v_\beta = A_\beta\omega_\beta\cos(\omega_\beta t_0) = \sqrt{3}\beta_0\omega_\beta$.

In this case, the timing error can be estimated as

$$\Delta_t^\beta = -\frac{2\Delta_\beta}{v_\beta} = \frac{\sin(2\beta_0)}{\sqrt{3}\beta_0\omega_\beta}\tan^2\alpha. \tag{13}$$

It was shown previously [14] that a timing error in the amplitude timing directly translates into an error in the amplitude estimate (calculated according to (3)):

$$\frac{\Delta A}{A} = \frac{\Delta_t}{T_\beta\tan(\pi(1/2 - t_A/T))}. \tag{14}$$

For the case of $\beta_0 = A_\beta/2$, we have $t_A = (4/12)T_\beta$ and obtain

$$\frac{\Delta A_\beta}{A_\beta} = \frac{\Delta_t^\beta}{T_\beta\tan(\pi/6)} = \frac{\sin(A_\beta)\tan^2(\alpha)}{\pi A_\beta}, \tag{15a}$$

$$\Delta A_\beta = \frac{1}{\pi}\sin(A_\beta)\tan^2(\alpha). \tag{15b}$$

For the other axis, we can deduce a corresponding error Δ_α:

$$\Delta_\alpha \sim \frac{1}{4}\sin(4\alpha_0)(\cos\beta - 1). \tag{16}$$

And as a consequence an error in timing if $\alpha_0 = A_\alpha/2$ is

$$\Delta_t^\alpha = \frac{2\Delta_\alpha}{v_\alpha} = \frac{2\Delta_\alpha}{\sqrt{3}\alpha_0\omega_\alpha} = \frac{1}{1}\frac{\sin(4\alpha_0)(\cos\beta - 1)}{\sqrt{3}\alpha_0\omega_\alpha} \tag{17}$$

and the corresponding error in estimated amplitude is

$$\Delta A_\alpha = \frac{-4\Delta_\alpha}{T_\alpha\omega_\alpha} \sim -\frac{\sin(2A_\alpha)(\cos\beta - 1)}{2\pi}. \tag{18}$$

In summary we have obtained the expressions which describe the deviation in measured timings due to the pin-cushion distortion from projecting the reflected beam on a flat surface. From this we also got an estimate for the resulting error in the estimation for the amplitude of the mirror motion.

3.2. Dynamic Projection. Now in a projector or scanner application, a Lissajous pattern is projected, which is displayed in Figure 6.

The projection onto a screen leads to coupling of the two motions, even in the absence of any physical interaction. In this case, when performing the timing measurements for one axis at a given deflection, also the deflection of the orthogonal axis at this moment has to be taken into account, which influences the results.

When using these timing values to estimate the amplitude based on a simple bisinusoidal model (corresponding to Figure 6(a)), we will obtain a certain (finite) number of different, slightly erroneous values, because we do not measure the ideal Lissajous figure, but rather the projection onto the plane of detection.

Let us first look at the timing measurement of horizontal deflection, that is, for the angle β. Here we have to consider a timing error (i.e., a deviation in the measured timing from the value, which would be expected in the case that $\alpha = 0$) $\Delta_t = (\Delta_\beta^1 + \Delta_\beta^2)/v$, where Δ_β^1 and Δ_β^2 are the errors in the measured timings during the forward and back transition of the beam over the diode. (They have to be summed up, because the movement is in opposite directions between two successive passages over the trigger diode.) Note that now Δ_β^1 and Δ_β^2 are different because the angles of the other axes, $\alpha(t_1)$ and $\alpha(t_2)$, are different at the two transitions over the photodiode. t_1, t_2 are the times when the beam hits the photodetector.

Using the same assumption as above ($\beta_0 = A_\beta/2$), we have $t_1 = \pi/6\omega_\beta$ and $t_2 = 5\pi/6\omega_\beta$ and, as a consequence, $\alpha(t_1) = A_a\sin((\omega_\alpha/\omega_\beta)(\pi/6 + 2n\pi) + \varphi)$ and $\alpha_2(t_2) = A_a\sin((\omega_\alpha/\omega_\beta)(5\pi/6 + 2n\pi) + \varphi)$.

The error in the amplitude timing is

$$\Delta t_\beta = -\frac{(\Delta_\beta^1 + \Delta_\beta^2)}{v_\beta} = \frac{\sin(2\beta_0)}{2\sqrt{3}\beta_0\omega_\beta}(\tan^2\alpha_1 + \tan^2\alpha_2). \tag{19}$$

Correspondingly, for the motion around the orthogonal axis, we obtain $\Delta t_\alpha = \sin(4A_\alpha)(2 - (\cos\beta_1 + \cos\beta_2))/2\sqrt{3}\alpha_0\omega_\alpha$.

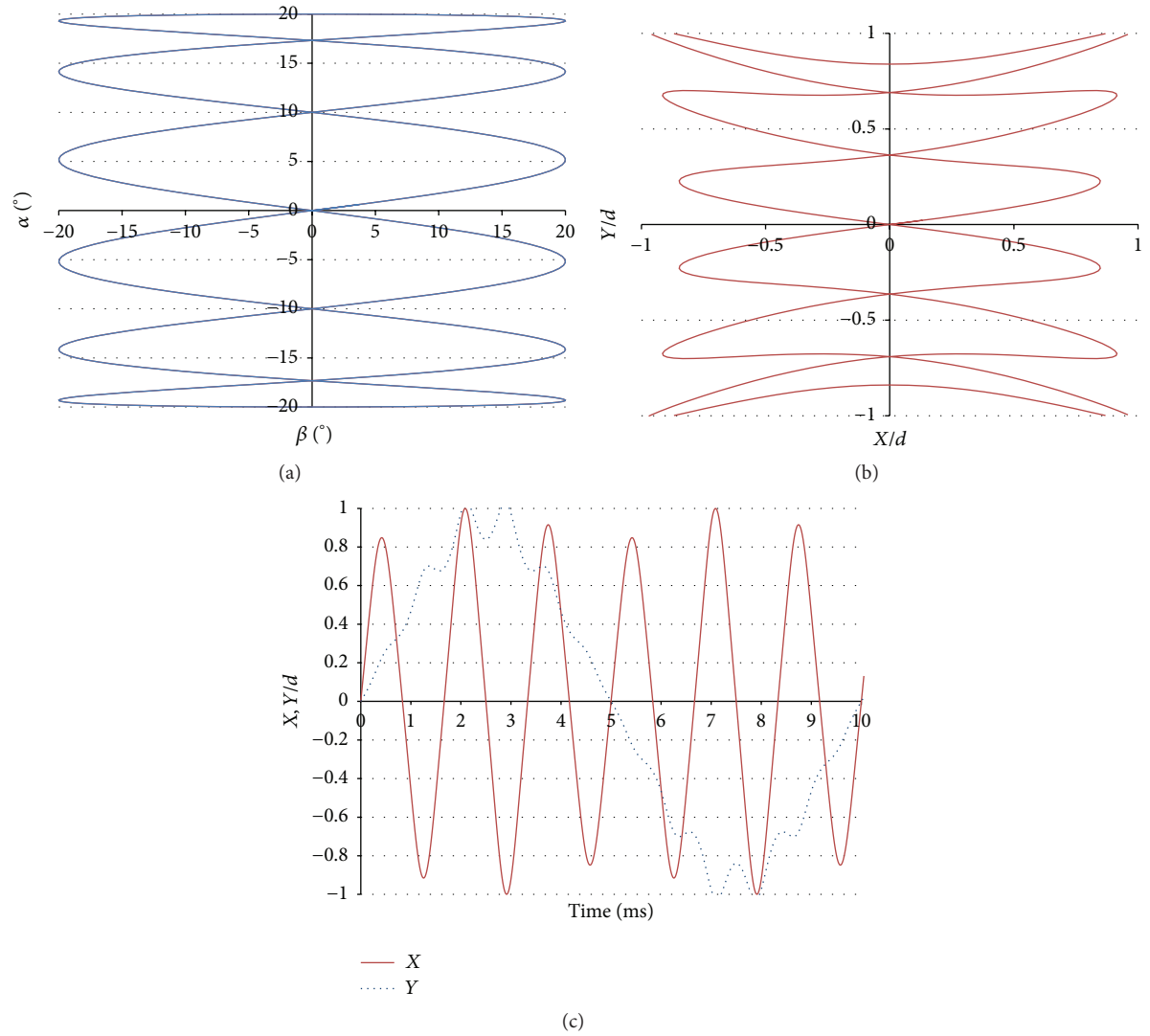

Figure 6: (a) The sinusoidal motion of the tilt angles corresponds to an ideal Lissajous pattern. (b) The projection onto a flat surface induces distortion. (c) This is reflected by a cross talk between x- and y-position on the screen, when plotted as a function of time. (Parameters for frequency and amplitude are similar to Table 1.)

Table 1: Parameters used for simulations.

Mechanical amplitude	$\alpha = \beta = 20^\circ$
Frequency ratio	$\omega_a : \omega_b = 6 : 1$
Detector position	$\alpha_0 = \beta_0 = 10^\circ$
Relative phase	$\varphi = 0^\circ$
Frequencies	$f_\alpha = 600$ Hz $f_\beta = 100$ Hz

4. Results for Given Conditions

Exemplarily, we assume the test-case shown in Table 1.

In this special case, the measurement of the deflection angle β exactly occurs at a point of zero transition of the orthogonal axis. Thus there is no timing error for the vertical axis.

Table 2: Estimated parameters for the test-case described in Table 1. For comparison, in the last column, numerically calculated values for the estimated time delay are shown.

N	β_1 (°)	β_2 (°)	Δt_α (μs)	$\Delta t_\alpha / t_\alpha$	t_α (ms)	$t_\alpha^{\text{num.}}$ (ms)
0	1.74	8.45	4.89	0.88%	0.5604	0.5606
1	18.13	19.92	47.30	8.51%	0.6029	0.6037
2	16.38	11.47	26.17	4.71%	0.5817	0.5824
3	−1.74	−8.45	4.89	0.88%	0.5604	0.5606
4	−18.13	−19.92	47.30	8.51%	0.6029	0.6037
5	−16.38	−11.47	26.17	4.71%	0.5817	0.5824

On the other hand, for the measurement of the amplitude of α, we have to take into account all the above considerations. The results are summarized in Table 2.

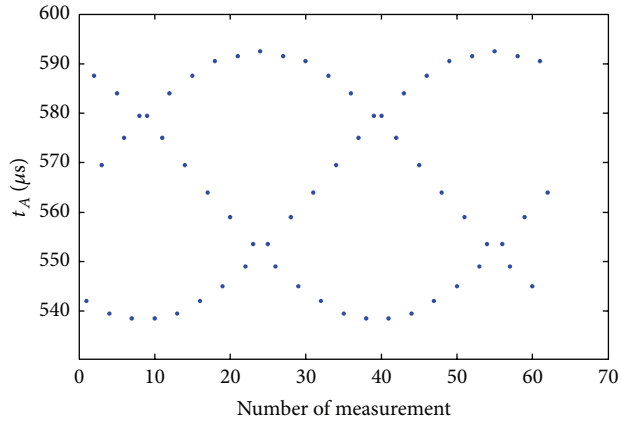

FIGURE 7: Timing values for measuring the amplitude of the fast axis for a frequency ratio of 62 : 10.

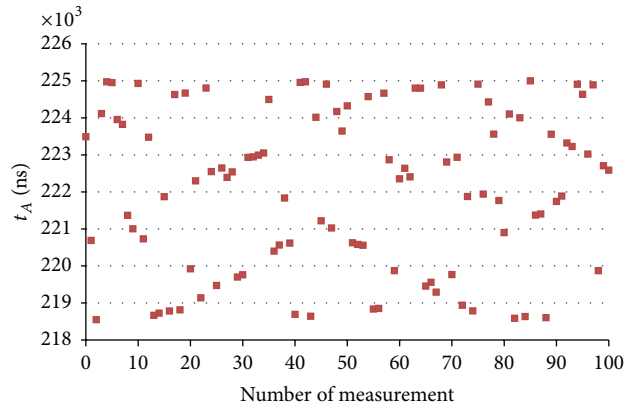

FIGURE 8: Modulated signals in the amplitude timing.

From the results shown in Table 2, we find excellent agreement of our analytical estimations with results from a numerical simulation of the mirror oscillation. The values deviate slightly due to the approximations in our derivation.

We see that timing errors on the order of some percent can occur for the case of mirror amplitude of 20°.

As a consequence, even in the absence of any noise sources, we do not obtain a single timing value, but rather a series of well-defined timing measurements, from which the amplitude can be calculated.

The number of discrete values depends on the frequency ratio between the two axes. In the simple example given here, it would be 3 different values. That is because of the simplicity of the Lissajous figure. For different frequency ratios, and, in particular, if the frequencies are not carefully adjusted so that their ratio corresponds to a rational number, we obtain a Lissajous figure which does not repeat itself and we get a continuous distribution of timing values.

In Figure 7, the calculated t_A-values are shown for a frequency ratio of $f_\alpha : f_\beta = 6.2 : 1.0$, which corresponds to a small mismatch.

In this case, the projected Lissajous figure does not stay constant but rather is slowly moving and repeats itself only after 10 periods.

Qualitatively, this behaviour was verified in our device as shown in Figure 8. Note that currently, due to limitations in the electronics, not every timing value is measured and evaluated, so there is systematic undersampling of the data. The important point in this case is the fact that the values fluctuate regularly in a range of about 5%, which corresponds well to the estimations above, which confirms the origin of these experimental results.

5. Conclusions and Outlook

In this paper, we reviewed our concept for position detection of the harmonic motion of electrostatically driven 2D MOEMS mirrors. A detailed analytical description of the timing signals observed was presented. It was shown that a cross talk between the two axes occurs, which must be considered for accurate amplitude measurements. The results from this analysis are confirmed by experimental results.

This cross talk leads to fluctuations in the amplitude signal on the order of several percent. For more accurate and faster amplitude measurements, these findings must be included in position detection devices based on timing measurements.

Conflict of Interests

The author declares that there is no conflict of interests regarding the publication of this paper.

Acknowledgments

The Competence Centre CTR is funded within the R&D Program COMET (Competence Centers for Excellent Technologies) by the Federal Ministries of Transport, Innovation and Technology (BMVIT) and of Economics and Labour (BMWA) and it is managed on their behalf by the Austrian Research Promotion Agency (FFG). The Austrian provinces (Carinthia and Styria) provide additional funding.

References

[1] M. E. Motamedi, Ed., *MOEMS: Micro-Opto-Electro-Mechanical Systems*, SPIE Press, 2005.

[2] S. T. S. Holmström, U. Baran, and H. Urey, "MEMS laser scanners: a review," *Journal of Microelectromechanical Systems*, vol. 23, no. 2, Article ID 6714402, pp. 259–275, 2014.

[3] C. Winter, L. Fabre, F. Lo Conte et al., "Micro-beamer based on MEMS micro-mirrors and laser light source," *Procedia Chemistry*, vol. 1, no. 1, pp. 1311–1314, 2009.

[4] A. D. Yalçınkaya, H. Urey, D. Brown, T. Montague, and R. Sprague, "Two-axis electromagnetic microscanner for high resolution displays," *Journal of Microelectromechanical Systems*, vol. 15, no. 4, pp. 786–794, 2006.

[5] F. Zimmer, H. Grueger, A. Heberer, A. Wolter, and H. Schenk, "Development of a NIR microspectrometer based on a MOEMS scanning grating," in *MEMS, MOEMS, and Micromachining*, vol. 5455 of *Proceedings of SPIE*, p. 9, Strasbourg, France, April 2004.

[6] U. Hofmann, J. Janes, and H.-J. Quenzer, "High-Q MEMS resonators for laser beam scanning displays," *Micromachines*, vol. 3, no. 2, pp. 509–528, 2012.

[7] B. Borovic, A. Q. Liu, D. Popa, H. Cai, and F. L. Lewis, "Open-loop versus closed-loop control of MEMS devices: choices and issues," *Journal of Micromechanics and Microengineering*, vol. 15, no. 10, pp. 1917–1924, 2005.

[8] A. Tortschanoff, M. Lenzhofer, A. Frank et al., "Position encoding and phase control of resonant MOEMS mirrors," *Sensors and Actuators A*, vol. 162, no. 2, pp. 235–240, 2010.

[9] A. Tortschanoff, A. Frank, M. Wildenhain, T. Sandner, and A. Kenda, "Optical position encoding and phase control of an electrostatically driven two-dimensional MOEMS scanner at two resonant modes," *Journal of Micro/ Nanolithography, MEMS, and MOEMS*, vol. 10, no. 3, Article ID 033006, 2011.

[10] H. Schenk, P. Dürr, D. Kunze, and H. Kück, "A new driving principle for micromechanical torsional actuators," in *Proceedings of the International Mechanical Engineering Congress and Exposition (MEMS '99)*, vol. 1, pp. 333–338, Nashville,Tenn, USA, 1999.

[11] A. Wolter, H. Schenk, E. Gaumont, and H. Lakner, "Improved layout for a resonant 2D micro scanning mirror with low operation voltages," in *MOEMS Display and Imaging Systems*, vol. 4985 of *Proceedings of SPIE*, p. 72, January 2003.

[12] H. Schenk, P. Dürr, T. Haase et al., "Large deflection micromechanical scanning mirrors for linear scans and pattern generation," *IEEE Journal on Selected Topics in Quantum Electronics*, vol. 6, no. 5, pp. 715–722, 2000.

[13] Antriebsprinzip zur Erzeugung resonanter Schwingungen von beweglichen Teilen mikromechanischer Bauelemente, European Patent EP 1 123 526 B1.

[14] A. Tortschanoff, M. Baumgart, A. Frank et al., "Optical position feedback for electrostatically driven MOEMS scanners," in *MOEMS and Miniaturized Systems XI*, vol. 8252 of *Proceedings of SPIE*, San Francisco, Calif, USA, January 2012.